ORIGINAL ARTICLE

Activation of CD8$^+$ T Cells in Chronic Obstructive Pulmonary Disease Lung

Ana B. Villaseñor-Altamirano[1,5*], Dhawal Jain[6*], Yunju Jeong[1,5], Jaivardhan A. Menon[1], Mari Kamiya[1,5], Hibah Haider[1], Reshmi Manandhar[1], Muhammad Dawood Amir Sheikh[1], Humra Athar[1,6], Louis T. Merriam[1], Min Hyung Ryu[2,5], Takanori Sasaki[3,5], Peter J. Castaldi[2,5], Deepak A. Rao[3,5], Lynette M. Sholl[4,5], Marina Vivero[4,5], Craig P. Hersh[2,5], Xiaobo Zhou[2,5], Justus Veerkamp[7‡], Jeong H. Yun[2,5‡], Edy Y. Kim[1,5‡], and the MGB-Bayer Pulmonary Drug Discovery Lab

[1]Division of Pulmonary and Critical Care Medicine, [2]Channing Division of Network Medicine, and [3]Division of Rheumatology, Inflammation, and Immunity, Department of Medicine, and [4]Department of Pathology, Brigham and Women's Hospital, Boston, Massachusetts; [5]Harvard Medical School, Boston, Massachusetts; [6]Pulmonary Drug Discovery Laboratory, Pharmaceuticals Research and Development, Bayer US LLC, Boston, Massachusetts; and [7]Pharmaceuticals, Research & Early Development Precision Medicine RED (preMED), Pharmaceuticals Research and Development, Bayer AG, Wuppertal, Germany

ORCID IDs: 0000-0002-3940-5617 (A.B.V.-A.); 0000-0001-9437-7201 (D.J.); 0000-0002-0453-3475 (Y.J.); 0000-0002-2093-3823 (M.K.); 0000-0001-5041-1068 (H.H.); 0009-0005-9938-6410 (R.M.); 0000-0002-5029-4161 (M.D.A.S.); 0000-0002-3731-6792 (L.T.M.); 0000-0003-3071-7363 (M.H.R.); 0000-0001-9672-7746 (D.A.R.); 0000-0001-7176-679X (M.V.); 0000-0002-1342-4334 (C.P.H.); 0000-0002-7127-2869 (X.Z.); 0000-0002-4361-8295 (J.H.Y.); 0000-0002-9095-3109 (E.Y.K.).

Abstract

Rationale: Despite the importance of inflammation in chronic obstructive pulmonary disease (COPD), the immune cell landscape in the lung tissue of patients with mild-moderate disease has not been well characterized at the single-cell and molecular level.

Objectives: To define the immune cell landscape in lung tissue from patients with mild-moderate COPD at single-cell resolution.

Methods: We performed single-cell transcriptomic, proteomic, and T-cell receptor repertoire analyses on lung tissue from patients with mild-moderate COPD ($n = 5$, Global Initiative for Chronic Obstructive Lung Disease I or II), emphysema without airflow obstruction ($n = 5$), end-stage COPD ($n = 2$), control ($n = 6$), or donors ($n = 4$). We validated in an independent patient cohort ($N = 929$) and integrated with the *Hhip*$^{+/-}$ murine model of COPD.

Measurements and Main Results: Mild-moderate COPD lungs have increased abundance of two CD8$^+$ T cell subpopulations: cytotoxic KLRG1$^+$TIGIT$^+$CX3CR1$^+$ TEMRA (T effector memory CD45RA$^+$) cells, and DNAM-1$^+$CCR5$^+$ T resident memory (T_{RM}) cells. These CD8$^+$ T cells interact with myeloid and alveolar type II cells via *IFNG* and have hyperexpanded T-cell receptor clonotypes. In an independent cohort, the CD8$^+$KLRG1$^+$ TEMRA cells are increased in mild-moderate COPD lung compared with control or end-stage COPD lung. Human CD8$^+$KLRG1$^+$ TEMRA cells are similar to CD8$^+$ T cells driving inflammation in an aging-related murine model of COPD.

Conclusions: CD8$^+$ TEMRA cells are increased in mild-moderate COPD lung and may contribute to inflammation that precedes severe disease. Further study of these CD8$^+$ T cells may have therapeutic implications for preventing severe COPD.

Keywords: chronic obstructive pulmonary disease; memory T cells; RNA sequence analysis; proteomics; multiomics

(Received in original form May 28, 2023; accepted in final form September 27, 2023)

*These authors contributed equally to this work.

‡These authors contributed equally to this work.

A complete list of MGB-Bayer Pulmonary Drug Discovery Lab members may be found in the supplement.

Supported by NIH Clinical Center grant K08HL146972, American Heart Association grant 867587, Bayer, and a Shore Faculty Development Award.

Author Contributions: This study was conceived, designed, and supervised by J.V., J.H.Y., and E.Y.K. The clinical study was supervised by J.H.Y. and E.Y.K. Clinical enrollment, phenotyping, and tissue sample processing was designed and performed by Y.J., J.A.M., M.K., H.H., R.M., M.D.A.S., H.A., L.M.S., and M.V. and supervised by E.Y.K. Bioinformatics analyses were performed by A.B.V.A., D.J., and J.H.Y.; assisted and reviewed by M.H.R., T.S., P.J.C., D.A.R., and C.P.H.; and supervised by J.H.Y. and E.Y.K. The manuscript was written by A.B.V.A., D.J., L.T.M., J.H.Y., and E.Y.K. and revised by M.H.R., P.J.C., C.P.H., X.Z., and J.V. Project administration was by E.Y.K.

This article has a related editorial.

Am J Respir Crit Care Med Vol 208, Iss 11, pp 1177–1195, Dec 1, 2023

Originally Published in Press as DOI: 10.1164/rccm.202305-0924OC on September 27, 2023
Internet address: www.atsjournals.org

At a Glance Commentary

Scientific Knowledge on the Subject: Although $CD8^+$ T cells are known to be increased in number in chronic obstructive pulmonary disease (COPD) lung, the immunophenotype of $CD8^+$ T cells and their association with disease severity are incompletely defined. Single-cell studies to date have not used a multiomic approach to immunophenotype T cells in COPD lung.

What This Study Adds to the Field: This study represents, to our knowledge, the first study performing multiomic single-cell analysis of lung tissue from patients with COPD and emphysema without airway obstruction. This study identifies increased abundance of a $CD8^+$ T-cell subpopulation ($KLRG1^+$ T effector memory $CD45RA^+$ [TEMRA] cells) in mild-moderate COPD lung. Our approach highlights the need for future studies comparing milder and end-stage COPD lung via multiomic approaches optimized for T cells.

Chronic obstructive pulmonary disease (COPD) has a complex pathobiology, including epithelial and endothelial injury leading to airway inflammation and alveolar destruction (i.e., emphysema) (1–3). Progression from mild to severe disease is highly variable and dependent on multiple factors, including environmental toxins, smoke inhalation, genetics, and the immune response. Compared with asymptomatic smokers, patients with COPD have amplified inflammation, and evidence suggests $CD8^+$ T cells play a central role (4). After antigen encounter, naive $CD8^+$ T cells undergo clonal expansion and differentiation into effector cells. A fraction of effector cells become memory T cells with specialized functions, such as circulating effector memory (T_{EM}) cells, tissue-resident memory (T_{RM}) cells, and terminally differentiated effector memory T cells expressing CD45RA (TEMRA). Given the distinct functions of $CD8^+$ T-cell subpopulations, understanding the $CD8^+$ T-cell state in COPD may offer insights into pathogenesis and therapeutic targets. Conventional immunophenotyping by flow cytometry shows shifts toward $CD8^+$ effector memory phenotypes. However, comprehensive and consistent immunophenotyping of $CD8^+$ T cells in COPD has been challenging because of variations in study design and patient characteristics, such as disease severity.

Single-cell RNA-sequencing (scRNA-seq) analysis of lungs explanted from patients with end-stage COPD have identified a range of cellular phenotypes, such as metabolic shifts and tolerance to oxidative stress in alveolar type II (AT2) cells (5). Studies of mild COPD have identified inflammatory cellular phenotypes, particularly in myeloid cells, and apoptosis among alveolar epithelial cells (6). Notably, in-depth characterization of $CD8^+$ T cells, together with their correlation with disease severity, is limited. Studies combining single-cell transcriptomics and proteomics have identified lymphoid subsets in other lung diseases (7–10) but have not been performed in COPD. Here, we use a single-cell, multiomic approach to characterize the $CD8^+$ T-cell phenotypes that distinguish mild-moderate COPD lung (scheme, Figure 1A). We found two $CD8^+$ T-cell subpopulations that were more abundant in mild-moderate COPD lung tissue. We then examined the gene signatures of these $CD8^+$ T-cell subpopulations in a larger, independent cohort of patients with COPD and an experimental murine model of COPD. Some of the results have been previously reported in abstract form (11).

Methods

Study Cohorts

Patients undergoing video-assisted thoracoscopic surgery for resection of nonmetastatic lung masses from April 2017 to December 2020 were enrolled with informed consent under protocols approved by the Brigham and Women's Hospital Institutional Review Board (2011P002419, 2014P002558, and 2019P003592). Excess, noncancerous lung parenchymal tissue was taken >2 cm from the tumor margin. Review of the electronic health record classified patients as control (absence of chronic lung disease), mild-moderate COPD (Global Initiative for Chronic Obstructive Lung Disease [GOLD] criteria I or II), or emphysema without airway obstruction (chest computed tomography imaging and histopathological evidence of emphysema and spirometry without airway obstruction) (Table 1 and Figure 1A). Emphysema was determined by the clinical reports by thoracic radiologists, which were in concordance with assessment in a blinded fashion by a board-certified pulmonary physician. These patients undergoing video-assisted thoracoscopic surgery were compared with lungs explanted from donors or patients undergoing lung transplant for end-stage COPD, of whom one subject had concurrent pulmonary fibrosis.

scRNA-Seq, CITE-Seq, and T-Cell Receptor Repertoire Analysis of Lung Tissue

Live cells from cryopreserved lung tissue were sorted by flow cytometry and stained with cellular indexing of transcriptomes and epitopes (CITE-seq) antibodies for single-cell proteomic analysis (12). Sequencing, demultiplexing, and quality control were performed using standard pipelines (*see* supplemental Methods and Figure E1 in the online supplement). Principal component analysis and uniform manifold approximation and projection and place (UMAP) (13) were used for dimensionality reduction, and clusters were annotated per Adams and colleagues (14), Travaglini and colleagues (15), and Clustree (16). CITE-seq data were generated from 197 proteins and 7 isotype controls (Table E1). Our scRNA-seq dataset

Upon publication, deidentified expression data will be available indefinitely at GEO and code at a repository.

Correspondence and requests for reprints should be addressed to Edy Y. Kim, M.D., Ph.D., Brigham and Women's Hospital, Hale Building for Transformative Medicine, Room 3016-I, 60 Fenwood Road, Boston, MA 02115. E-mail: ekim11@bwh.harvard.edu.

This article has an online supplement, which is accessible from this issue's table of contents at www.atsjournals.org.

Table 1. Patient Cohort Demographics

	Control	Mild-Moderate COPD	Emphysema without Airway Obstruction	*P* Value
N	6	5	5	—
Age, yr	68 ± 9	71 ± 11	64 ± 8	0.68
Sex, % F	83	100	60	0.27
GOLD category				
I	—	2	—	—
II	—	3	—	—
BMI, kg/m^2	27 ± 4.4	27 ± 2.4	28 ± 3.9	0.66
Spirometry				
FEV_1% predicted	92 ± 18	78 ± 16	73 ± 23	0.36
FEV_1/FVC, %	72 ± 4	60 ± 6	70 ± 8	**0.0014**
Home oxygen	None	None	None	—
Smoking status				
Ever-smoker	2	5	5	**0.012**
Current smoker	1	3	2	0.33
Pack-years	9.3 ± 22	33 ± 12	45 ± 13	**0.038**
Inhaled medications				
Corticosteroid	1	1	1	0.99
Bronchodilator	2	2	2	0.97
Oral corticosteroids	0	0	1	0.31
Diagnosis of lung mass				
Malignant	5	5	4	0.59
Benign	1	0	1	—

Definition of abbreviations: BMI = body mass index; COPD = chronic obstructive pulmonary disease; GOLD = Global Initiative for Chronic Obstructive Lung Disease.
Data are shown as mean ± SD or *n*. Kruskal-Wallis testing for continuous variables (age, BMI, spirometry). Chi-square tests for categorical variables (sex, smoking status, medications, diagnosis of lung mass). Comparisons with *P* value < 0.05 are in boldface.

was integrated with two published scRNA-seq datasets: human lung from patients with end-stage COPD and donors published by Adams and colleagues (14) and our published dataset of murine lung from the *Hhip*$^{+/-}$ model of COPD (17). Single-cell dataset is available at https://zenodo.org/record/8393742.

Validation in the Lung Tissue Research Consortium

We used gene expression signatures for CD8$^+$KLRG1$^+$ TEMRA cells (163 genes) and T_{RM}1 cells (178 genes) on 929 samples from the Lung Tissue Research Consortium (LTRC) (supplemental Methods) (18). We used the HALLMARK IFNγ-response gene set (200 genes). Genes that overlapped with the CD8$^+$ T-cell clusters were removed. We used the gene set variation analysis pipeline (19) in batch-adjusted, normalized, length-scaled counts per million.

Results

T-Cell Populations in COPD Lung

We performed single-cell transcriptomic (scRNA-seq) and proteomic (scCITE-seq, 197 targets; Table E1) analysis of lung tissue from surgical resections of nonmetastatic lung masses in patients with mild-moderate COPD (GOLD I or II, $n = 5$), emphysema without airway obstruction ($n = 5$), or control subjects ($n = 6$), with comparison to lung explanted from donors ($n = 4$) or patients with end-stage COPD ($n = 2$) (Figure 1A and Tables 1 and E2). In our scRNA-seq and CITE-seq dataset, 109,361 cells passed quality control (Figure E1). Our multiomic analysis (Figure 1B) included 71 high-resolution clusters: 7 endothelial, 11 epithelial, 35 lymphoid, 4 mesenchymal, and 14 myeloid (Figures E2 and E3 and Table E3). This multiomic study with a large panel of antibodies against cell surface markers demonstrated several advantages over using only RNA-seq. We identified markers for immune cell subsets and their activation even if the corresponding RNA was scarcely expressed or post-transcriptionally modified. We identified 35 lymphoid cell subsets with high resolution, such as TEMRA cells defined by protein expression of CD45RA, a splice variant not typically captured with scRNA-seq.

Lung tissue from surgical resection of lung masses (i.e., control, mild-moderate COPD, and emphysema without obstruction) had increased relative abundance of lymphoid cells and decreased myeloid cells compared with lungs explanted for lung transplantation (i.e., donor and end-stage COPD) (Figure E4A). Resected lung tissue was procured >2 cm from the tumor margin, but the immune compartment may still be affected. Alternatively, explanted lung tissue (i.e., donor and end-stage COPD) experienced mechanical ventilation and longer postsurgical ischemic time. Hence, "control" lung tissues were the key comparison to mild-moderate COPD, as both were taken during resection of lung masses.

The relative abundance of CD8$^+$ T cells was increased in mild-moderate COPD lung tissue compared with lung from other patient subcohorts (Figure E4B). By annotating clusters using both transcriptomic and proteomic markers (Figures 1B and 1C), we identified 10 CD8$^+$ T-cell subclusters: two TEMRA, five T_{RM}, T_{EM}, γδ T cell, and mucosal-associated invariant T cells. The five CD8$^+$ T_{RM} clusters were distinguished by levels of *GZMB* expression and by transcriptional or protein expression of these genes: CD8$^+$ T_{RM} cluster 1 (*IL7R*$^+$, *ANXA1*$^+$), T_{RM}2 (*IL7R*$^+$, *XCL1*$^+$), T_{RM}3 (CD94$^+$, CD56$^+$), T_{RM}4 (*IL7R*[lo], CD5$^+$), and T_{RM}5 (*IL7R*$^+$, CD41$^+$) (Figures 1C and E3 and Table E3).

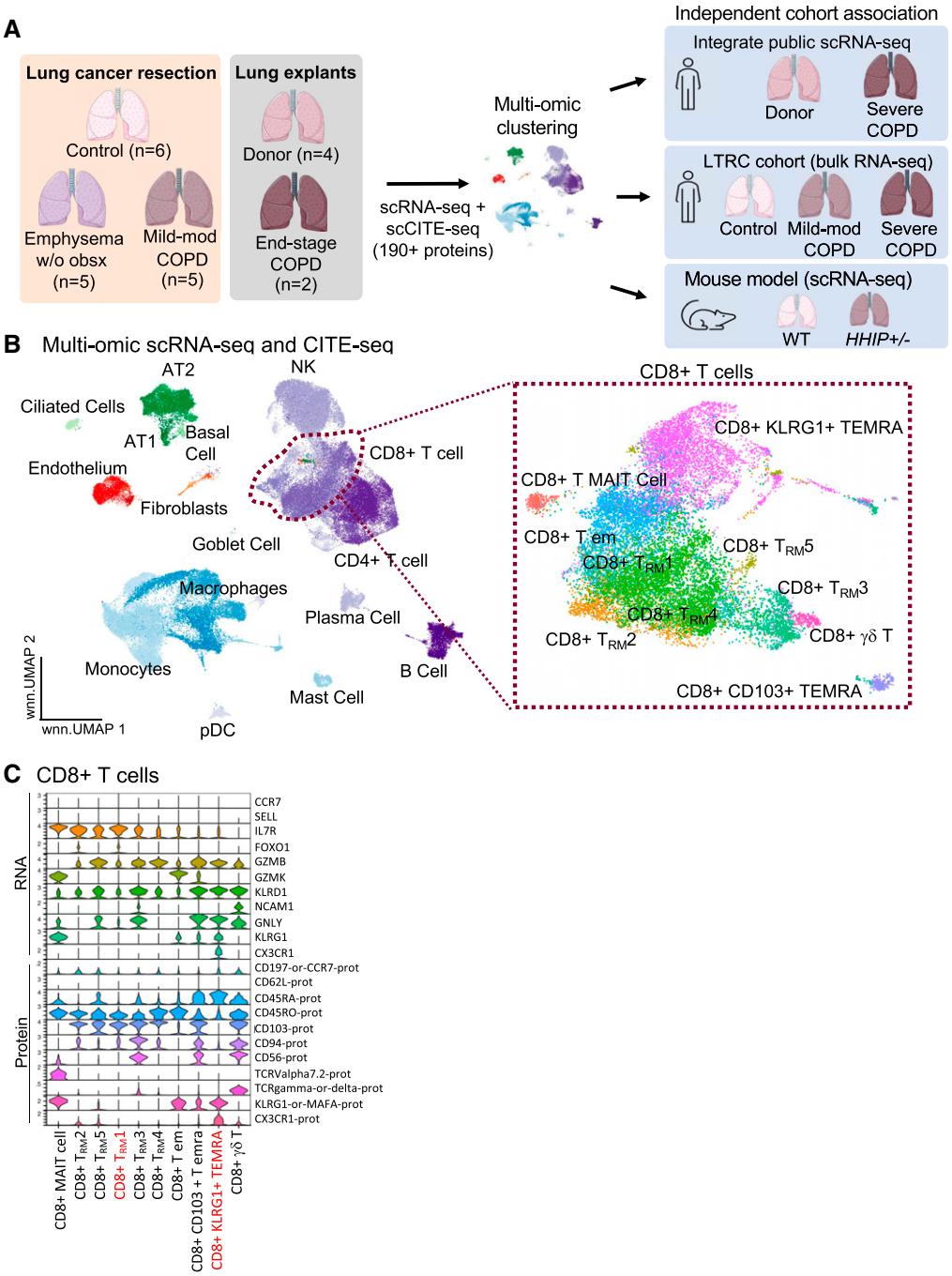

Figure 1. CD8$^+$ T effector memory CD45RA$^+$ (TEMRA) and T resident memory (T_{RM}) cells have increased abundance in mild-moderate chronic obstructive pulmonary disease (COPD) lung. (*A*) Study approach. Lung tissues surgically resected from patients without chronic lung disease (control), mild-moderate COPD, or emphysema without airway obstruction (emphysema w/o obsx) were compared with lungs from explanted "donors" and patients undergoing lung transplantation for COPD (end-stage COPD). Single-cell transcriptomic and proteomic analyses of these lung tissues were compared with independent patient cohorts and a murine model of COPD. (*B–D*) Single-cell RNA-sequencing (scRNA-seq) and scCITE-seq analysis of lung tissue. (*B*) UMAP visualization of cell clusters; inset: CD8$^+$ T-cell clusters. (*C*) Transcriptional and protein markers defining CD8$^+$ T-cell clusters. Red indicates cell clusters enriched in mild-moderate COPD compared to other patient subcohorts. (*D*) Relative abundance of cell clusters in pairwise comparison of patient subcohorts using the scCODA computational pipeline; red indicates cell clusters enriched in the red subcohort compared with control or donor. (*E*) Relative abundance of cell clusters in mild-moderate COPD tested by the MiloR computational pipeline; red indicates clusters enriched compared with control. AT2 = alveolar type II; CITE-seq = cellular indexing of transcriptomes and epitopes; NK = natural killer.

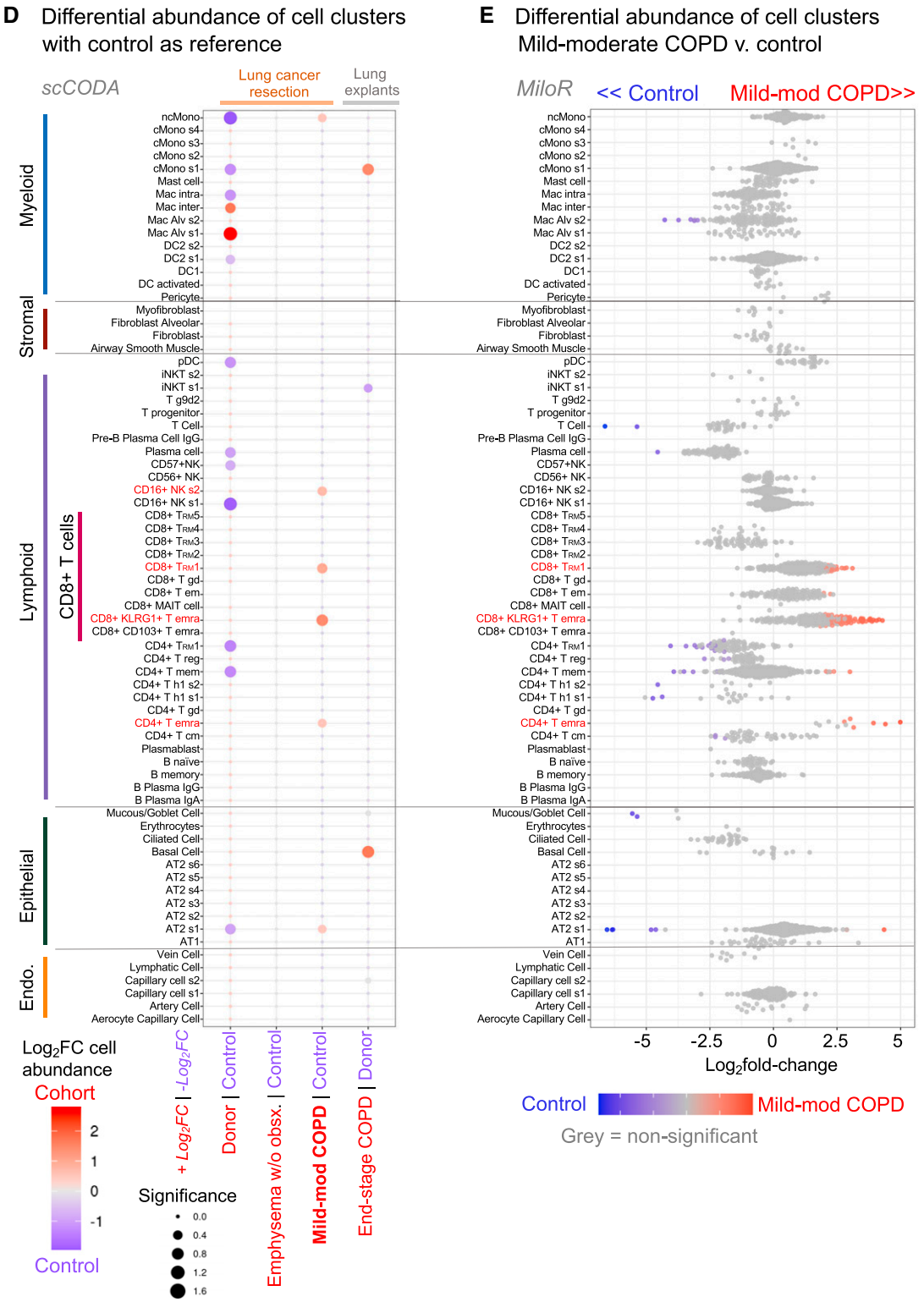

Figure 1. (*Continued*).

We tested the relative abundance of the 71 cell clusters in a pairwise comparison of patient subcohorts using the Bayesian statistical approach of the scCODA computational pipeline (Figure 1D). We found three T-cell subclusters—$CD8^+KLRG1^+$ TEMRA cells, $CD8^+$ $T_{RM}1$ cells, and $CD4^+$ TEMRA cells—were increased in abundance in mild-moderate COPD lung compared with control lung (red, Figures 1D and 1E). A different statistical approach, k-nearest neighbor in the miloR computational pipeline, confirmed this result (Figure 1E). Going forward, we focused on the two most abundant CD8 T-cell populations, $CD8^+KLRG1^+$ TEMRA and $CD8^+$ $T_{RM}1$ cells. In mild-moderate COPD lung, $KLRG1^+$ TEMRA and $T_{RM}1$ $CD8^+$ T cells comprised a median of 6.7% and 8.6% of total cells, a significant difference compared with other patient subcohorts (Kruskal-Wallis test, adjusted [adj.] $P = 0.015$ and 0.098, respectively) (Tables 2 and E4). The relative abundance of $CD8^+KLRG1^+$ TEMRA cells and $CD8^+$ $T_{RM}1$ in mild-moderate COPD lung were increased 4.4-fold and 5.6-fold (adj. $P = 0.017$ and 0.095, respectively), compared with control lung (Tables 2 and E4 and Figure E4). $CD4^+$ TEMRA cells comprised only 0.4% of total cells in mild-moderate COPD lung tissue.

$CD8^+$ TEMRA and T_{RM} Cell Immunophenotypes in Mild-Moderate COPD

In the single-cell proteomic dataset, expression of natural killer (NK) cell–related markers distinguished $CD8^+$ TEMRA ($KLRG1^+$, $CD57^+$) from $CD8^+$ $T_{RM}1$ cells ($CD94\ [KLRD1]^+$, $NKG2D^+$) (Figures 2A and 2B and Table E3). These $CD8^+$ T-cell subpopulations also had distinct immune checkpoint phenotypes, with $CD8^+KLRG1^+$ TEMRA cells expressing TIGIT and $CD8^+$ $T_{RM}1$ expressing DNAM-1 (CD226) and TACTILE (CD96). Similarly, their chemokine receptors were distinct, with $CD8^+KLRG1^+$ TEMRA cells expressing CX3CR1, whereas $CD8^+$ $T_{RM}1$ cells were $CCR5^+$. As expected, $CD8^+$ $T_{RM}1$ cells had increased protein expression of markers of tissue residency, such as CD103 (integrin αE), CD49a (integrin β1) (20), and CD69 (Figures 2A and 2B and Table E3).

We next examined the global transcriptome (RNA-seq) to gain insight into candidate functions of these $CD8^+$ T cells (Figures 2C, 2D and E5). $KLRG1^+$ TEMRA cells upregulated expression of the transcription factors *ZEB2* (which cooperates with t-bet to promote terminal differentiation of cytotoxic T cells [21]) and *KLF2*, a transcription factor that drives quiescence (22–24). $CD8^+KLRG1^+$ TEMRA cells showed enriched expression of the gene set for cytotoxicity (Figures 2E and E6), cytotoxic genes such as *GZMA*, *GZMB*, *GZMH* (25), *GNLY*, and *PRF1*, and cytotoxicity-related genes, such as *EOMES* (26, 27), *KLRC4*, and *KLRD1* (Figures 2C, 2D, and E5). $KLRG1^+$ TEMRA cells also had enriched expression of *ADGRG1* (alias *GPR56*) (28) and *CST7* (cystatin F), possible negative regulators of cytotoxic cells (29) (Figure E5 and Table E3). In contrast to $KLRG1^+$ TEMRA cells, $T_{RM}1$ cells had increased expression of genes associated with inflammation (e.g., *ANXA1*, *XCL1*), and long-term memory–related gene set (Figure 2E) and genes like *IL7R*, *FOXO1*, and *PARP8* (30) (Figures 2C, 2D, and E5). In summary, distinct immunophenotypes for $CD8^+$ T cells in COPD include cytotoxic, $CX3CR1^+TIGIT^+KLRG1^+$ TEMRA cells, and inflammatory $CCR5^+DNAM\text{-}1^+TACTILE^+$ $T_{RM}1$ cells.

Expansion of $CD8^+$ T-Cell Receptor Clonotypes in Mild-Moderate COPD

To better understand the dynamics of $CD8^+$ T-cell differentiation, we examined the T-cell receptor (TCR) clonotypes in our single-cell analysis. TCR clonotypes are the unique TCR sequences generated by VD(J) recombination, which underlies the diversity of antigen specificities for TCRs. Mild-moderate COPD lung tissue had a trend for the lowest diversity of unique TCR clonotypes, as measured by the Shannon index (Figure 2F) (Kruskal-Wallis, $P = 0.029$; *post hoc* pairwise adj. $P = 0.075$, compared with control). In mild-moderate COPD lung tissue, $KLRG1^+$ TEMRA cells shared TCR clonotypes with $CD8^+$ T_{EM} cells. $T_{RM}1$ cells shared clonotypes with several other resident memory subpopulations (Figure 2G).

This reduced diversity of TCR sequences measured by the Shannon index (Figure 2F) is in line with the hyperexpansion of specific TCR clonotypes in mild-moderate COPD lung. Hyperexpanded TCR clonotypes shared by at least 100 T cells comprised 10.4% of T cells (588 cells) in mild-moderate COPD lung (Figures 2H and E7 and Table E3). Only 5.0% of T cells (122 cells) were hyperexpanded in control lung, and no TCR clonotypes were hyperexpanded in patients with emphysema without airway obstruction. Within mild-moderate COPD lung tissue, the hyperexpanded TCR clonotypes were in the $KLRG1^+$ TEMRA and $T_{RM}1$ cells (Figure 2I), and this hyperexpansion of a minority of clonotypes contributed to their increased abundance overall.

$CD8^+$ T Cells and Inflammatory Pathways in Mild-Moderate COPD

The CellChat computational pipeline (31) identified the cell types interacting with $CD8^+$ T cells. In mild-moderate COPD lung, $CD8^+KLRG1^+$ TEMRA and $T_{RM}1$ cell clusters had the strongest and most numerous outgoing interactions, which can be the production of secreted ligands like cytokines (*x*-axis in Figure 3A, right). In contrast, these $CD8^+$ T cells were not among the top 25 clusters for outgoing interactions in control lung (*x*-axis in Figure 3A, left). In mild-moderate COPD lung, classical or nonclassical monocytes/macrophages (cMono or ncMono), classical dendritic cells (cDC2),

Table 2. Selected T-Cell Populations in Lung Tissue

	Donor	Control	Emphysema without Airway Obstruction	Mild-Moderate COPD	End-Stage COPD
$CD8^+KLRG1^+$ TEMRA	1.9 (0.1–4.8)	1.4 (0.4–6.3)	1.4 (0.4–2)	6.7 (2.5–27)	1.8 (0.8–2.9)
$CD8^+$ $T_{RM}1$	1.9 (1.5–4.5)	0.9 (0.3–3.9)	0.9 (0.2–5.7)	8.6 (0.4–11)	3.9 (1.5–6.4)
$CD4^+$ TEMRA	0 (0–0.1)	0.8 (0–1.9)	0.1 (0–0.3)	0.4 (0.1–10.9)	0.2 (0–0.4)

Definition of abbreviations: COPD = chronic obstructive pulmonary disease; TEMRA = T effector memory $CD45RA^+$; $T_{RM}1$ = T resident memory 1. Data are shown as median percentage of total cells (range).

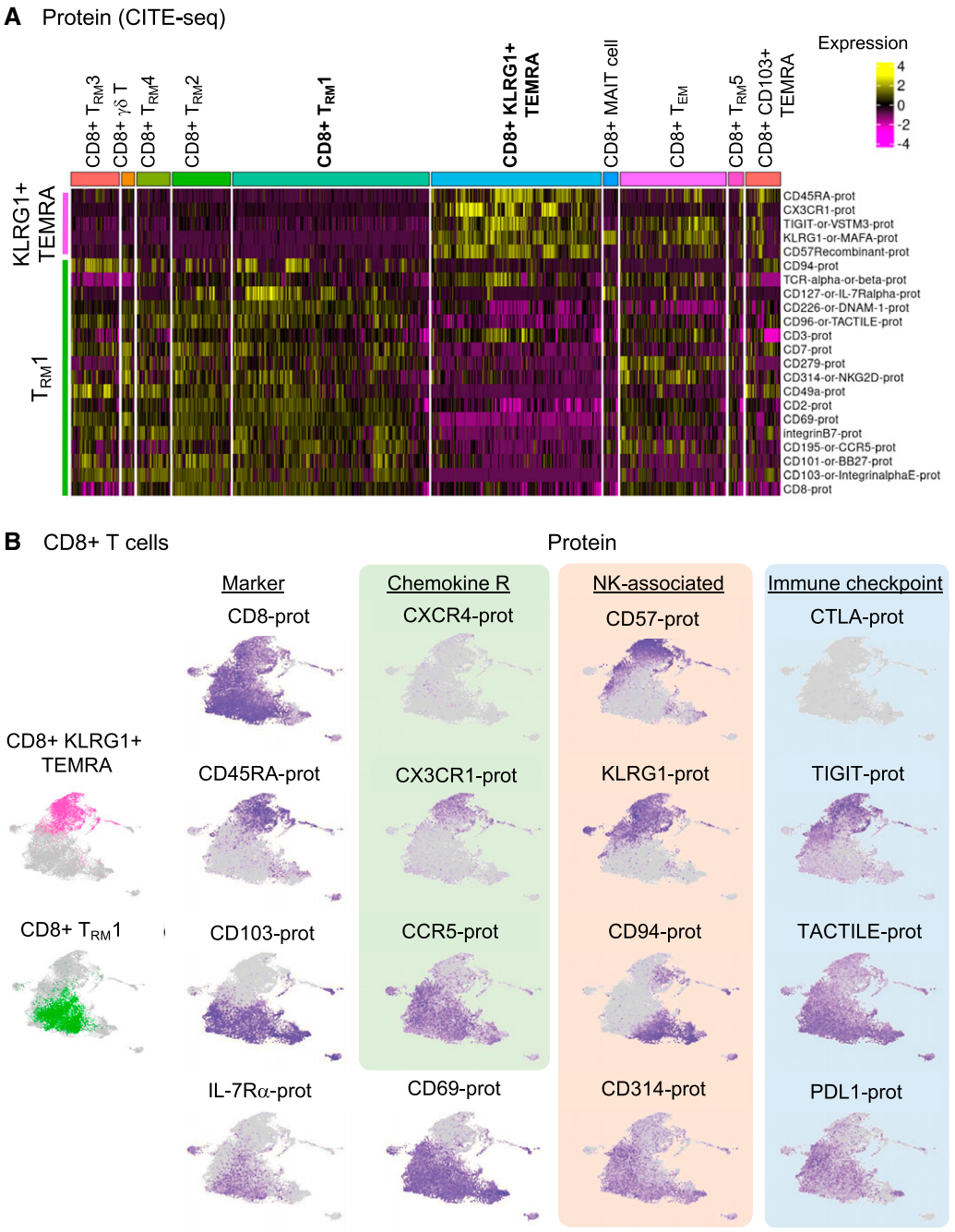

Figure 2. $CD8^+KLRG1^+$ T effector memory $CD45RA^+$ (TEMRA) and T resident memory 1 ($T_{RM}1$) cells have distinct immunophenotypes in mild-moderate chronic obstructive pulmonary disease (COPD) lung. $CD8^+$ T-cell clusters are examined in the multiomic integration of single-cell RNA-seq, CITE-seq, and T-cell receptor (TCR) sequence repertoire analysis of lung tissue. (*A–E*) Lung tissue from mild-moderate COPD is examined. (*A* and *B*) CITE-seq dataset of protein expression. (*A*) Heatmap of proteins differentially expressed in $CD8^+KLRG1^+$ TEMRA and $T_{RM}1$ cells, by $CD8^+$ T cell cluster. (*B*) UMAP visualization of differentially expressed proteins. (*C–E*) RNA-seq dataset of mRNA expression. (*C*) Heatmap of transcripts differentially expressed in $CD8^+KLRG1^+$ TEMRA and $T_{RM}1$ cells, by $CD8^+$ T cell cluster. (*D*) UMAP visualization of differentially expressed genes. (*E*) UMAP visualization of differentially expressed pathways and associated genes. (*F*) Boxplot of clonotype diversity measured by Shannon index by patient (dot) and grouped by subcohort. (*G*) The sharing of TCR clonotype among $CD8^+$ T cell clusters in mild-moderate COPD lungs. (*H* and *I*) Each $CD8^+$ T cell is classified by its clonotypic expansion, ranging from single T cell with a specific clonotype to hyperexpanded (>100 T cells with same TCR clonotype). The proportion of $CD8^+$ T cells in each classification is shown by: (*H*) patient subcohort; and (*I*) $CD8^+$ T-cell cluster within mild-moderate COPD lung tissue. Emphysema w/o obsx = emphysema without airway obstruction; NK = natural killer.

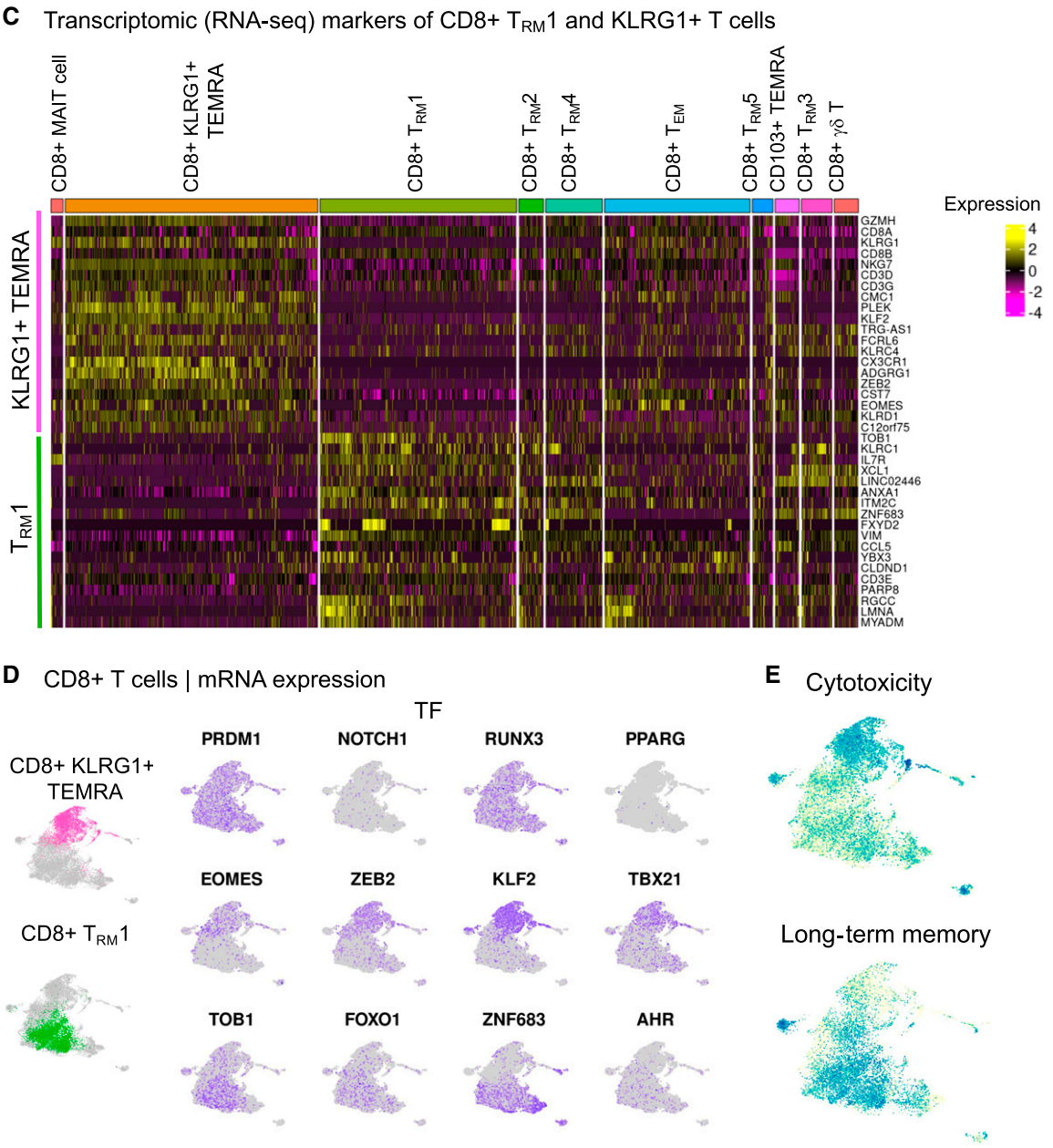

Figure 2. (*Continued*).

and AT2 cells were the four top clusters for incoming interactions, such as receptors for cytokines or chemokines (*y*-axis in Figure 3A, right). The main cellular targets for $CD8^+$KLRG1$^+$ TEMRA and T_{RM}1 cells were cMono, ncMono, cDC2 s1 (CD1c-prot$^+$, FceRIa-prot$^+$, CD45RO-prot$^+$, *AREG*$^+$, *CLEC10A*$^+$, *PLD4*, *CCL5*$^-$), and AT2 s1 (LAMP1-prot$^+$, *HHIP*$^+$, *SERPINA1*$^+$) cells (Figure 3B). Compared with control lung, KLRG1$^+$ TEMRA and T_{RM}1 cells had increased outgoing proinflammatory signals in mild-moderate COPD (Figure 3C). Both $CD8^+$ T-cell subpopulations had increased inflammatory axes, such as *ANNEXIN*, *IFNG*, *TNF*, and *TWEAK* (a pluripotent TNF-family cytokine [32]), together with *TGFB*, in mild-moderate COPD (Figure 3C). We corroborated this interactome analysis with the NicheNet algorithm (33), choosing $CD8^+$ T-cell subpopulations as the "sending" cells (Figure 3D). As with CellChat, this approach highlighted *IFNG* and *TNF* axes directed toward myeloid and AT2 cells (Figures 3D and E8).

Our interactome analysis suggested that $CD8^+$ T cells communicate with myeloid and AT2 cells via IFNγ. We next identified the dominant sources of *IFNG*. $CD8^+$KLRG1$^+$ TEMRA and T_{RM}1 cells were the leading senders of *IFNG* signaling in mild-moderate COPD lung (Figure 3E), whereas myeloid and AT2 cells were the

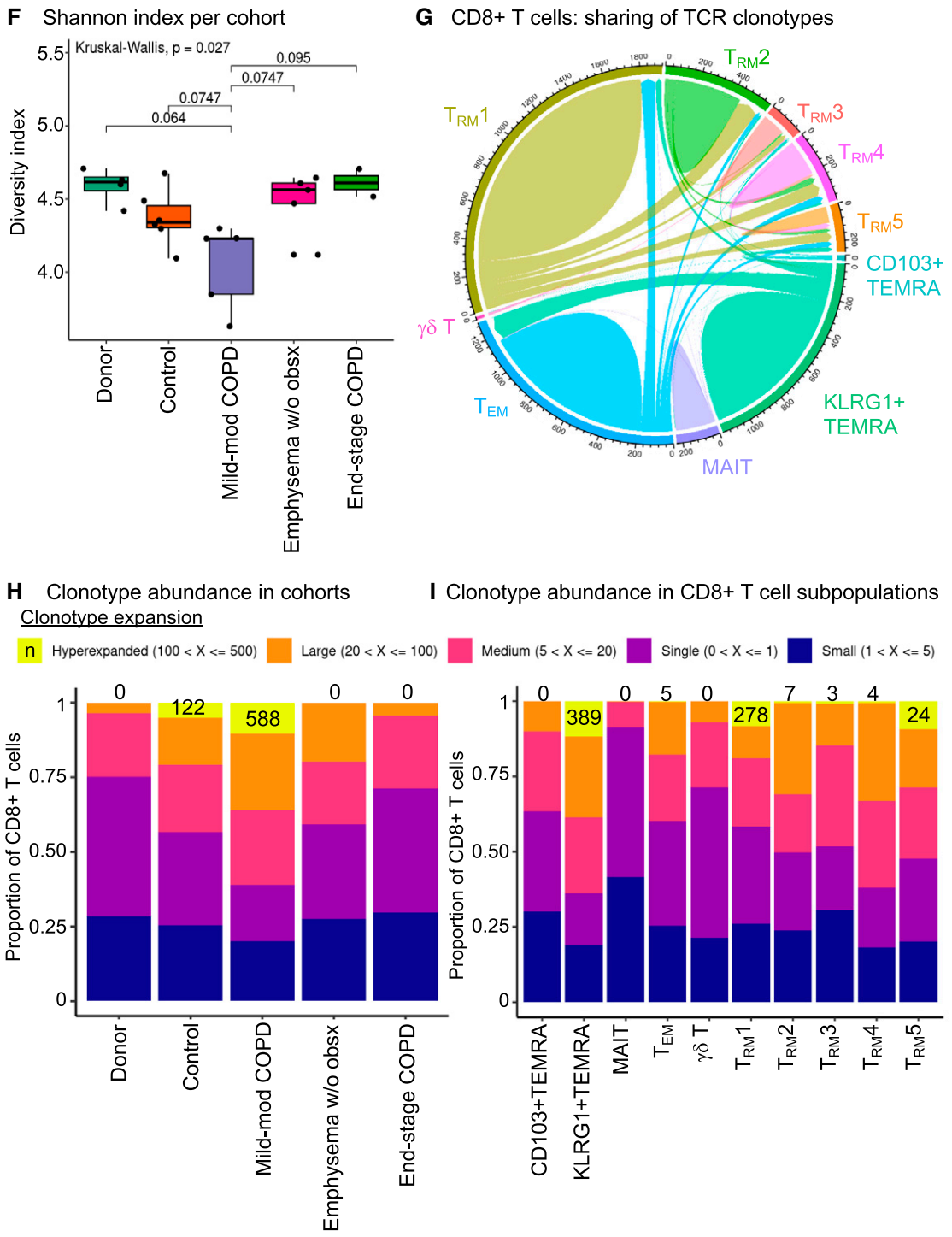

Figure 2. (*Continued*).

major targets ("receivers") of *IFNG* signaling overall (Figure 3E) and from $CD8^+KLRG1^+$ TEMRA and $T_{RM}1$ cells specifically (Figure 3F). We next examined the reverse direction signals sent by myeloid cells toward $CD8^+$ T cells (Figures E9A and E9B). Myeloid cells send signals known to drive production of *IFNG*, such as *IL12B* and *IL15*, to $KLRG1^+$ TEMRA and $T_{RM}1$ cells (and IL-18 to $T_{RM}1$ cells only). Myeloid cells also had candidate interactions via noninflammatory axes like IL-10 and TGFB1. Finally, we examined candidate interactions between $KLRG1^+$ TEMRA and $T_{RM}1$ cells, which included *CCL5*, *FAS-FASL*, *IFNG*, *TNF*, *TGFB1*, and *TNFSF14* (LIGHT) axes (Figures E9C and E9D).

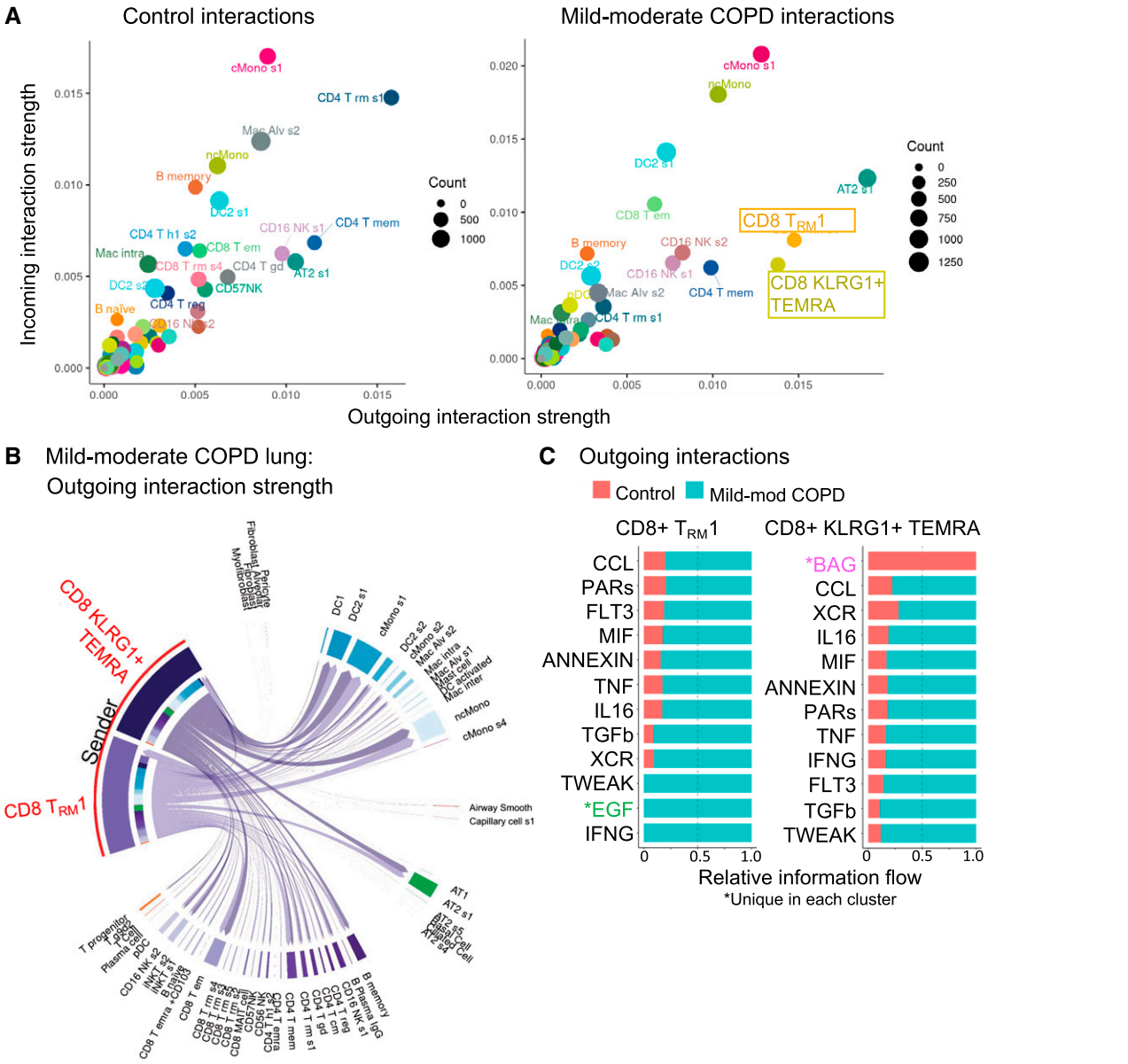

Figure 3. CD8$^+$ T cells interact with myeloid and alveolar type II (AT2) cells by inflammatory axes in mild-moderate chronic obstructive pulmonary disease (COPD) lung. Interactome analyses were performed on the single-cell RNA-sequencing (scRNA-seq) dataset of lung tissue from the control or mild-moderate COPD patient subcohorts. (*A–C*, *E*, and *F*) Statistically significant interactions determined by the CellChat pipeline are shown. (*A*) Total strength of incoming (*y*-axis) and outgoing (*x*-axis) interactions for each cell cluster, by patient subcohort. (*B*) For CD8$^+$KLRG1$^+$ T effector memory CD45RA$^+$ (TEMRA) and T resident memory 1 (T$_{RM}$1) cells (red), outgoing interactions in mild-moderate COPD lung. Color density is proportional to interaction strength. Receiving cell color indicates lineage (lymphoid, purple; epithelial, green; myeloid, blue). (*C*) For CD8$^+$KLRG1$^+$ TEMRA and T$_{RM}$1 cells, the strongest outgoing interactions (and their relative strength in control versus mild-moderate COPD). *Unique in each cluster. (*D*) Interactions were tested by the Nichenet pipeline. Interactions increased in mild-moderate COPD lung compared with control lung with adjusted *P* value < 0.05 are shown. Sending cells are CD8$^+$KLRG1$^+$ TEMRA or T$_{RM}$1 cells. (Top) Receiving cells are pooled myeloid cells: classical (c) Monos (monocyte/macrophages), nonclassical (nc)Monos, and dendritic cells (DC2 cluster 1). (Bottom) Receiving cells are AT2 cluster 1. (*E*) For the *IFNG* signaling pathway in mild-moderate COPD lung, strength of incoming (*y*-axis) and outgoing (*x*-axis) interactions for each cell cluster. (*F*) For the *IFNG* signaling pathway, visualization of outgoing interactions from CD8$^+$KLRG1$^+$ TEMRA or T$_{RM}$1 cells. Thickness of arrows and the size of receiving clusters are proportional to interaction strength. NK = natural killer.

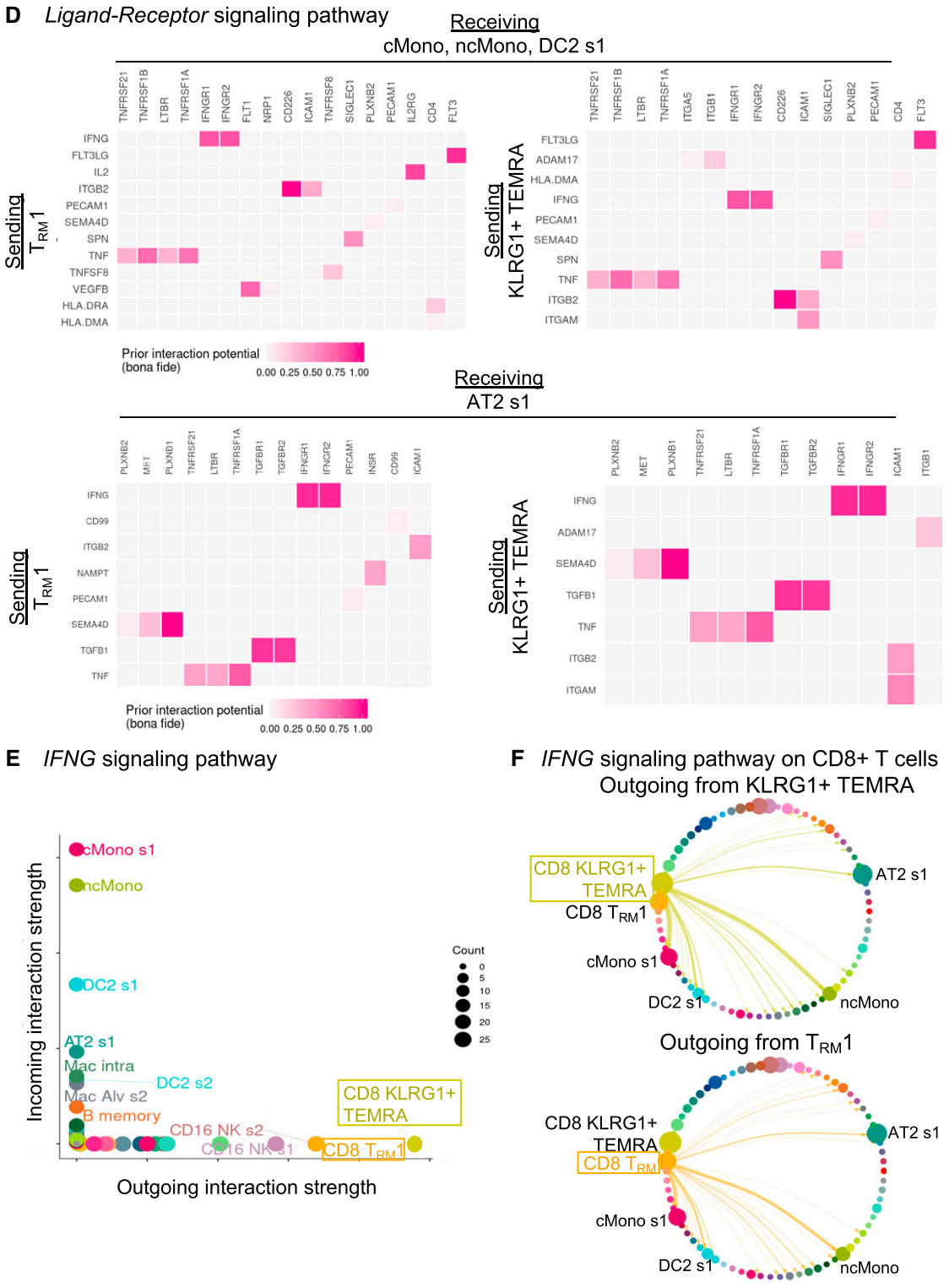

Figure 3. (*Continued*).

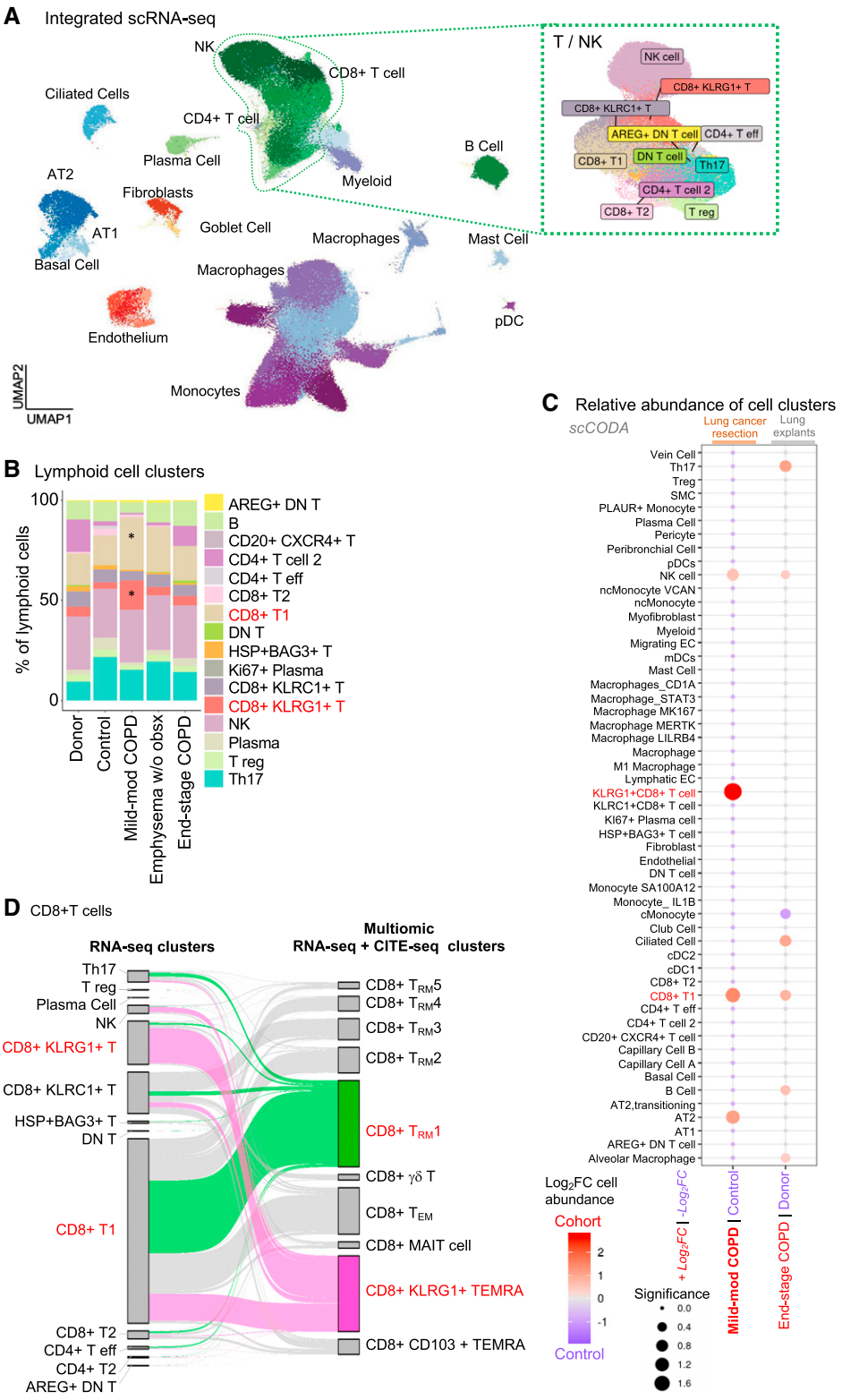

Figure 4. CD8$^+$*KLRG1*$^+$ T cells have increased abundance in mild-moderate chronic obstructive pulmonary disease (COPD) lung compared with end-stage COPD. Single-cell RNA-sequencing (scRNA-seq) datasets from this study and Adams and colleagues (14) were integrated. (*A*) UMAP visualization of cell clusters with lineage indicated by color. Green dotted line denotes natural killer (NK) and T-cell clusters. (*B*) Relative abundance of lymphoid clusters, by patient subcohort. *Indicates CD8$^+$ T1 (tan) and CD8$^+$KLRG1$^+$ (orange) T cells. (*C*) Relative abundance of cell clusters in pairwise comparison of patient subcohorts using the scCODA computational pipeline; red indicates cell clusters

Table 3. Lung Tissue Research Consortium Cohort Demographics

	Control	Mild-Moderate COPD	Severe COPD	*P* Value
n	346	327	256	
Age, yr	61.6 ± 12.5	67.8 ± 9.4	60.7 ± 8.2	<0.001
Male	136 (39.3)	197 (60.2)	131 (51.2)	<0.001
White race	312 (90.2)	303 (92.7)	230 (89.8)	0.54
Former smoker	199 (57.5)	254 (77.7)	222 (86.7)	<0.001
Smoking pack-years	20.2 (27.4)	47.0 (35.7)	44.4 (27.5)	<0.001
FEV_1% predicted	95.9 (12.6)	70.5 (16.3)	25.2 (9.1)	<0.001
GOLD category	0 (0)	1.65 (0.5)	3.7 (0.5)	<0.001

Definition of abbreviations: COPD = chronic obstructive pulmonary disease; GOLD = Global Initiative for Chronic Obstructive Lung Disease. Data show mean ± SD or *n* (%). *t* test for continuous variables (age, smoking pack-years, FEV_1). Chi-square tests for categorical variables (sex, smoking status, GOLD).

CD8$^+$ T Cells in Mild-Moderate and End-Stage COPD Lung

We next performed a more robust comparison of mild-moderate COPD lung and end-stage COPD lung. As published data for scCITE-seq of lung tissue from patients with COPD are not available, we integrated only our scRNA-seq results with 165,759 cells from the Adams and colleagues dataset (14) of explanted donor ($n = 15$) and end-stage COPD lung ($n = 17$) (Figure E10). We selected the Adams and colleagues dataset because the patients had been enrolled at our institution with a similar method, namely cryopreservation of samples before single-cell analysis. Integration of our and Adams and colleagues' scRNA-seq datasets demonstrated all major lineages and 53 clusters (Figures 4A, E11A, and E11B and Table E5). Among the 12 lymphoid cell subpopulations, CD8$^+$*KLRG1*$^+$ and CD8$^+$ T1 T cells were increased in mild-moderate COPD compared with other patient subcohorts (starred, Figure 4B). As in our multiomic analysis, lung tissue procured during surgical resection of a lung mass had an increased abundance of lymphoid cells compared with explanted lung, regardless of disease state (Figure E11C). Hence, when comparing multiple lineages, it was important to compare mild-moderate COPD and end-stage COPD to their respective comparison groups, "control" (from surgical resection of lung masses) or "donor" explanted lung. CD8$^+$*KLRG1*$^+$ T cells had increased relative abundance in mild-moderate COPD (compared with control), but CD8$^+$*KLRG1*$^+$ T cells were not more abundant in end-stage COPD compared with donors (scCODA algorithm, red text in Figure 4C; Figure E11D). The median percentage of CD8$^+$*KLRG1*$^+$ cells (among total lung cells) were: donor (0.4%), control (1.9%), mild-moderate COPD (5.8%), emphysema without airway obstruction (1.8%), and end-stage COPD (0.8%) (Table E6). The CD8$^+$ T1 cluster had a greater abundance in mild-moderate COPD (compared with control) than in end-stage COPD explant (compared with donor explant) (red in Figure 4C; Figure E11D). The median percentage of CD8$^+$ T1 cells (among total lung cells) were: donor (1.8%), control (8.3%), mild-moderate COPD (15.8%), emphysema without airway obstruction (9.4%), and end-stage COPD explant (4.2%) (Table E6).

We next defined the relationship between the cell clusters defined in our multiomic analysis (Figures 1–3) and the cell clusters defined in this analysis of only scRNA-seq (Figure 4A). The CD8$^+$*KLRG1*$^+$ T cells in the scRNA-seq–only analysis mapped nearly entirely to the CD8$^+$KLRG1$^+$ TEMRA cluster in the multiomic analysis (Figure 4D). CD8$^+$ T1 cells mapped to the $T_{RM}1$ cluster in the multiomic analysis. However, CD8$^+$ T1 cells also mapped to several other clusters in the multiomic analysis, including T_{RM}, T_{EM}, and the KLRG1$^+$ TEMRA cluster. This finding illustrated how multiomic analysis facilitated more fine clustering than RNA-seq only. In sum, the scRNA-seq–only analysis supported the increased relative abundance of CD8$^+$KLRG1$^+$ TEMRA cells in mild-moderate COPD lung compared with end-stage COPD. However, this RNA-seq–only analysis was unable to separate CD8$^+$ $T_{RM}1$ cells from other resident-memory T cells.

Validation of CD8$^+$ T Cell Gene Signatures in an Independent COPD Cohort

We validated our findings in a larger ($N = 929$) independent patient cohort, the LTRC (Table 3) (34) using bulk RNA-seq analysis of whole-lung tissue from patients with mild-moderate COPD (GOLD I or II), severe COPD (GOLD III or IV), or control. We generated marker gene scores for CD8$^+$KLRG1$^+$ TEMRA and $T_{RM}1$ cells using gene set variation analysis to estimate the abundance of CD8$^+$ T-cell subpopulations. The KLRG1$^+$ TEMRA score was increased in mild-moderate COPD lung compared with control (Kruskal-Wallis test, $P = 0.00061$; *post hoc* pairwise adj. $P = 4 \times 10^{-4}$). Although the mean TEMRA score was increased in mild-moderate compared with severe COPD lung, this difference was not significant (Figure 5A and Table E7). When divided by GOLD criteria, lung tissue from GOLD I or GOLD II patients had significantly increased KLRG1$^+$ TEMRA gene signature scores compared with control (Kruskal Wallis test, $P = 0.0049$; *post hoc* pairwise adj. $P = 0.014$ or

Figure 4. (*Continued*). enriched in COPD compared with their respective control. Red text highlight CD8$^+$*KLRG1*$^+$ and T1-cell clusters. (*D*) On the left, CD8$^+$ T cells in the scRNA-seq–only analysis (from Figure 4A) are mapped to themselves on the right in the multiomic (scRNA-seq/CITE-seq) analysis (from Figure 1B). The cell cluster annotations for either the RNA-seq only (left) or multiomic (right) analyses are shown. Cells in the KLRG1$^+$ T effector memory CD45RA$^+$ (TEMRA) and T resident memory 1 ($T_{RM}1$) multiomic clusters are highlighted as pink or green, respectively.

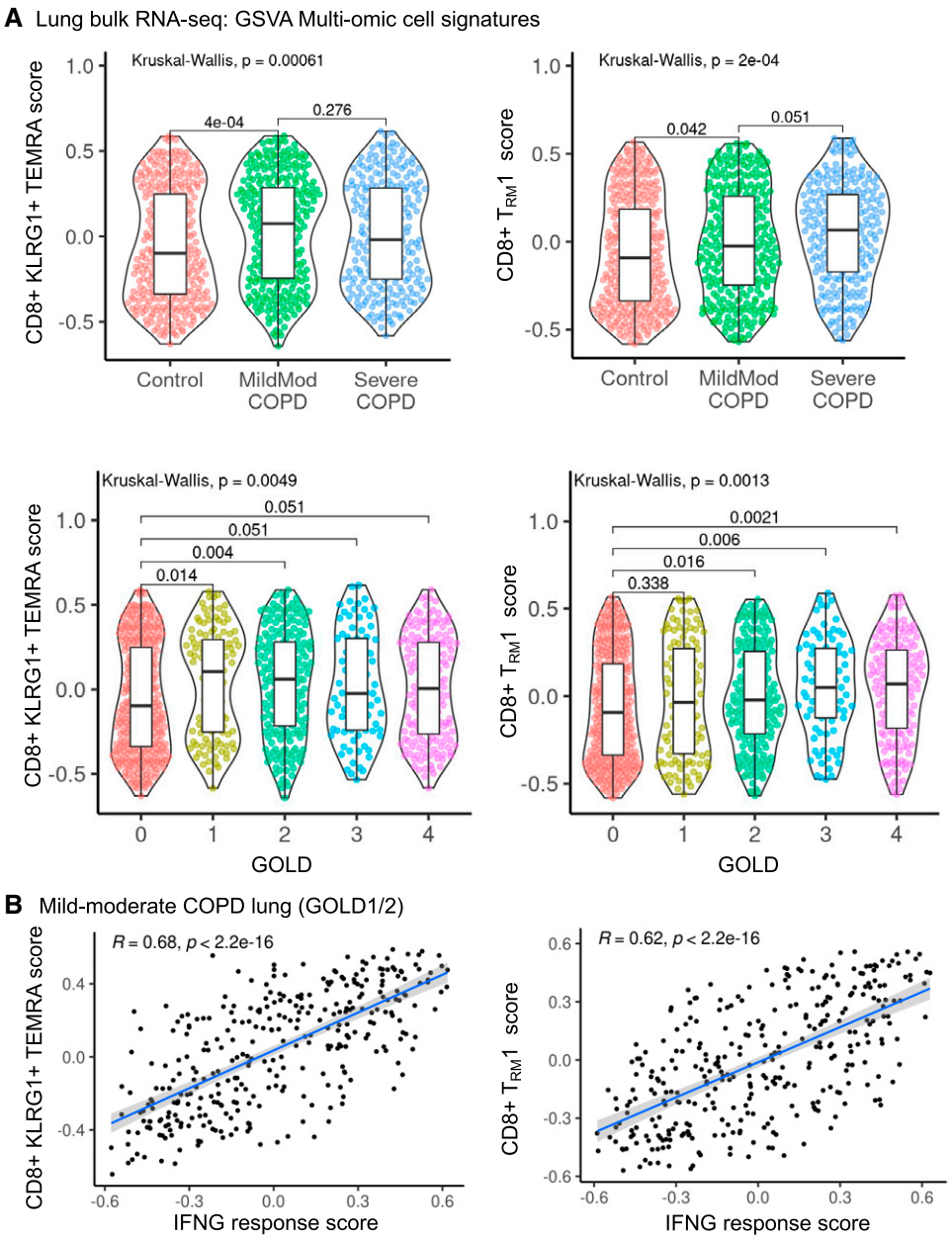

Figure 5. $CD8^+KLRG1^+$ T effector memory $CD45RA^+$ (TEMRA) and T resident memory 1 ($T_{RM}1$) cell gene signatures are increased in mild-moderate chronic obstructive pulmonary disease (COPD) lung in an independent cohort. Gene set variation analysis (GSVA) signature scores were generated for $CD8^+$ T-cell clusters from the single-cell datasets and measured in a bulk RNA-seq dataset of lung tissue from an independent patient cohort (Lung Tissue Research Consortium, $n = 929$) of control subjects and patients with COPD. (*A*) GSVA signature scores for $CD8^+$ T-cell clusters are shown by patient subcohort or Global Initiative for Chronic Obstructive Lung Disease (GOLD) classification. (*B*) In mild-moderate COPD lung, GSVA signature scores for $CD8^+$ T-cell clusters are compared with an IFNγ-response signature score. (*A*) Kruksal-Wallis with *post hoc* pairwise Wilcoxon testing with *P* values adjusted by multiple testing correction with Benjamini-Hochberg. (*B*) Pearson correlation with linear regression (blue line), 95% confidence interval (gray), correlation coefficient (*R*), and *P* values (*p*).

0.004, respectively) (Figure 5A). The $KLRG1^+$ TEMRA gene signature score only had a trend toward an increase in GOLD III or IV compared with control (*post hoc* pairwise comparison, adj. $P = 0.051$). From a multivariate linear regression analysis adjusted for age, sex, race, and smoking status, we found the $CD8^+KLRG1^+$ TEMRA gene signature was most strongly associated with mild-moderate COPD ($P = 0.009$) but also with severe COPD ($P = 0.014$), compared with control (Table E7). In summary, a large validation cohort confirmed that the $CD8^+KLRG1^+$ TEMRA gene signature is increased in mild-moderate COPD lung compared with control lung. This analysis in the LTRC cohort does not distinguish expression in mild-moderate

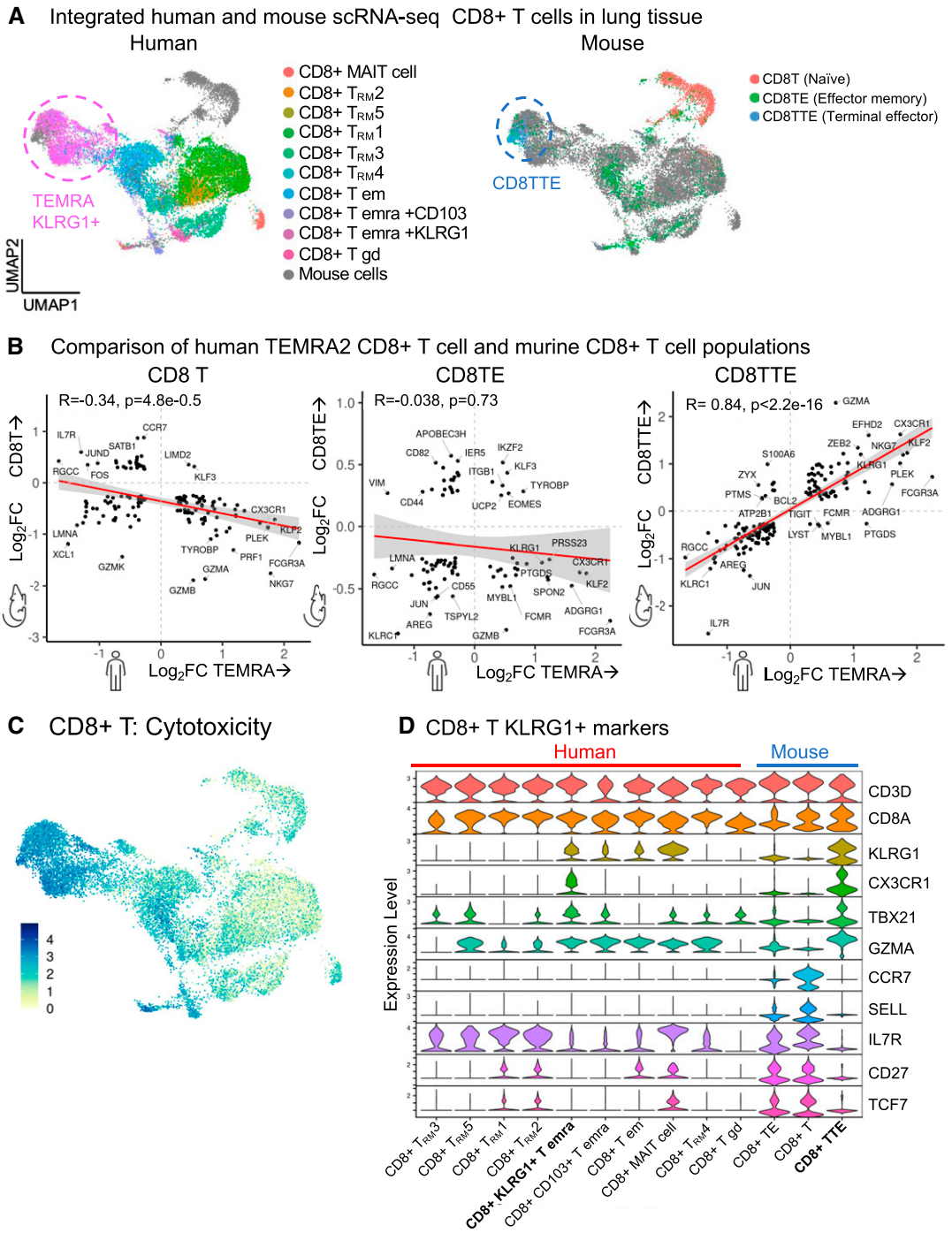

Figure 6. Comparative analysis of CD8$^+$ T cells. Single-cell RNA-sequencing (scRNA-seq) datasets of human CD8$^+$ T cells from this study and the *Hhip*$^{+/-}$ murine model of aging-associated chronic obstructive pulmonary disease (COPD) without smoke exposure (17) are compared. The human and murine datasets were integrated into one reference map. (*A*) Human (left) or murine (right) cells are mapped on UMAP visualizations of the integrated dataset. (*B*) Using pseudobulk analysis, the differentially expressed genes in murine CD8$^+$ T cell subpopulations (*y*-axis) are compared with the differentially expressed genes in human CD8$^+$KLRG1$^+$ T effector memory CD45RA$^+$ (TEMRA) cells (*x*-axis). For each CD8$^+$ T-cell population, gene expression is compared with all the other CD8$^+$ T cells in that human or murine dataset. Genes with $\log_2$fold-change (FC) > 0.25 and adjusted $P < 0.01$ are shown. (*C*) UMAP visualization of the cytotoxicity pathway. (*D*) Transcriptional expression of genes defining human and murine CD8$^+$ T cell clusters. (*B*) Spearman correlation with linear model (red), 95% confidence interval (gray), Spearman coefficient (r_s) and *P* value.

COPD compared with severe COPD. Because T cells corresponding to TEMRA cells were increased in abundance in mild-moderate COPD lung in our single-cell analyses (Figures 1 and 4), our findings in the LTRC cohort (Figure 5) may reflect the technical limits of identifying KLG1$^+$ TEMRA cells in whole-lung bulk RNA-seq rather than at single-cell resolution. Alternatively, the finding may reflect underlying biological variability in the association of KLRG1$^+$ TEMRA cells with disease severity.

The CD8$^+$ T_{RM}1 gene signature showed a significant positive association with COPD, with the gene signature score peaking in GOLD IV patients (Kruskal-Wallis test, $P = 0.0013$). Increased expression of the CD8$^+$ T_{RM}1 signature genes in both mild-moderate and severe COPD in this bulk RNA-seq analysis may reflect our earlier finding that the single-cell RNA-seq analysis did not distinguish among the multiple CD8$^+$ T_{RM} cell subpopulations identified by multiomic analysis (Figure 4D). In a multivariate linear regression model, the CD8$^+$ T_{RM}1 gene signature shows significant positive association with age, race, and severe COPD (GOLD III–IV) (Table E7).

Because CD8$^+$KLRG1$^+$ TEMRA cells and T_{RM}1 cells communicate with myeloid and AT2 cells via *IFNG* (Figure 3), we measured the association of their cellular gene signatures with an *IFNG* response score (Table E7). We excluded genes overlapping between the *IFNG* response score and the CD8$^+$ T cell signatures. The gene signatures for CD8$^+$KLRG1$^+$ TEMRA ($r = 0.68$, adj. $P = 2.2 \times 10^{-16}$) and CD8$^+$ T_{RM}1 cells ($r = 0.62$, adj. $P = 2.2 \times 10^{-16}$) were positively associated with *IFNG* response (Figure 5B).

Cross-Species Analysis Identifies Shared CD8$^+$ T Cytotoxic Cell Signature

To support future mechanistic studies, we turned to a murine model of COPD (17) driven by *Hhip* heterozygosity, a locus strongly associated with clinical COPD (35, 36). In this murine model, aging without smoke exposure results in emphysema and elevated airway resistance (17, 37) (Figure 6A). We assessed for similarities between human and murine CD8$^+$ T cells by integrating our human COPD lung scRNA-seq dataset with our previously published murine lung scRNA-seq dataset from the *Hhip*$^{+/-}$ model. On the shared human/mouse reference UMAP, we projected either the human CD8$^+$ T cells (Figure 6A, left) or murine CD8$^+$ T cells (Figure 6A, right). We annotated the human cells as in Figure 1, and we annotated the murine cells as in our previous publication (17): CD8T (naive), CD8TE (effector memory), and CD8TTE (terminal effector). On UMAP, human CD8$^+$KLRG1$^+$ TEMRA cells are adjacent and overlapping with murine CD8TTE cells. To confirm the transcriptional similarities between human and murine CD8$^+$ T cell subpopulations, we compared the differentially expressed genes in murine CD8$^+$ T cell subpopulations (*y*-axis, Figure 6B and Table E8) to the differentially expressed genes in human CD8$^+$KLRG1$^+$ TEMRA cells (*x*-axis, Figure 6B). Among murine CD8$^+$ T cells, only CD8TTE cells showed a positive correlation of their global transcriptome with that of human CD8$^+$KLRG1$^+$ TEMRA cells, with R = +0.84 ($P < 2.2 \times 10^{-16}$). Human CD8$^+$KLRG1$^+$ TEMRA and murine CD8TTE cells share differentially expressed genes associated with cytotoxicity (Figure 6C) and marker genes that we had identified for human KLRG1$^+$ TEMRA cells (Figure 2), such as *CX3CR1*, *KLF2*, *KLRG1*, and *ZEB2* (Figure 6D, volcano plots in Figure E12, and Table E8). In addition, human CD8$^+$KLRG1$^+$ TEMRA and murine CD8TTE cells share differential expression of *TBX21* (T-bet), the canonical transcription factor for *IFNG* production.

Discussion

To our knowledge, this is the first study to use single-cell multiomic analysis of lung tissue to comprehensively characterize CD8$^+$ T-cell states in COPD. We found increased abundance of CD8$^+$ T cells in lung tissue from patients with mild-moderate disease compared with control subjects and patients with end-stage COPD. On deep phenotyping, two subpopulations of CD8$^+$ cells, KLRG1$^+$ TEMRA and T_{RM}1, drove the increased number of CD8$^+$ T cells in mild-moderate COPD. Our results profiling CD8$^+$ T cells across stages of disease add to the myeloid and epithelial cell focus of single-cell RNA-seq studies to date (5, 6, 14, 38, 39). Our finding of increased CD8$^+$ TEMRA cells from COPD lungs adds to the previous investigations demonstrating increased CD8$^+$ TEMRA cells from COPD sputum, BAL, or blood. Findings in blood have been mixed, with some studies showing no differences, whereas recent phenotyping of peripheral blood (40) revealed CD8$^+$ TEMRA cells expressing KLRG1, similar to the CD8$^+$ TEMRA cells in our study. The discrepancies in the literature may stem from patient heterogeneity, such as smoking status or disease severity.

KLRG1 is expressed by many terminally differentiated cells and is classically an inhibitory receptor (40, 41). The expression of KLRG1 protein itself is not associated with the severity of airway obstruction (42). Because KLRG1 can be a marker of senescence or resistance to apoptosis (41,43,44), the hypothesis arises that the increase of KLRG1$^+$ TEMRA cells in mild-moderate COPD lung is driven by accumulation of longer-lived cells rather than proliferation. Alternatively, the hyperexpansion of a subset of TCR clonotypes could suggest the chronic antigenic stimulation seen in autoimmune diseases like systemic lupus erythematosus (45) and multiple sclerosis (46). The sharing of some TCR clonotypes supports the hypothesis that T_{EM} differentiated into TEMRA cells. The function of KLRG1$^+$ TEMRA cells in COPD is unclear. Given our immunophenotyping results, pathogenic roles for KLRG1$^+$ TEMRA cells could include direct cytotoxicity or activation of myeloid or AT2 cells to promote inflammation and tissue destruction. A key question is whether candidate inhibitory receptors on the TEMRA cells, like KLRG1$^+$ and the immune checkpoint receptor TIGIT, can be targeted to regulate the function of these cells. The cellular dynamics of T_{RM}1 cells may be more complex. The sharing of clonotypes among T_{RM} subpopulations raises the question whether different computational models might better reflect the underlying biology, or, alternatively, different local microenvironments might affect the transcriptomes and place a clonotype in multiple T_{RM} cell clusters.

Our interactome analysis highlighted IFNγ signaling axes for TEMRA and T_{RM} cells. Previous literature in clinical COPD demonstrated that CD8$^+$ T cells secrete IFNγ (42, 47), and CD8$^+$ T cells are enriched in preterminal and terminal bronchioles in COPD that upregulate IFNγ responses (38). In a series of elegant studies by Wang and colleagues, *Hhip* deletion in murine lung fibroblasts drives expansion in IFNγ$^+$ tissue-resident T cells, suppression of AT2 stem cell renewal, and histological changes of

emphysema. *Ex vivo* analysis demonstrated IFNγ secreted from explanted tissue-resident T cells mediate AT2 stem cell suppression (48). Without cigarette smoke exposure, *Hhip*$^{+/-}$ mice develop lung inflammation, emphysema, and elevated airway resistance with age (37). In the murine *Hhip*$^{+/-}$ model, KLRG1^{+}CD8TTE cells became more abundant with aging, produced IFNγ, and associated with lung emphysema (17). In our study, CD8^{+}KLRG1^{+} TEMRA cells in clinical COPD shared transcriptomic similarity to these KLRG1^{+}CD8TTE cells in *Hhip*$^{+/-}$ mice. These prior studies and our comparative analysis support the *Hhip*$^{+/-}$ mouse as a tool to dissect the role of CD8^{+}KLRG1^{+} TEMRA cells and specific genes (such as KLRG1 itself) in COPD. More generally, because *HHIP* is strongly associated with clinical COPD in genome-wide association studies, combining immunophenotyping of clinical COPD and the *Hhip*$^{+/-}$ murine model could illustrate how a genetic locus without an *a priori* immune function can influence the immune response.

There are limitations to our study. First, we have a low number of subjects, a reflection of the inherent difficulties in procuring mild to moderate COPD lung tissue. To gain new insights from a limited patient subcohort, we compared emphysema without airway obstruction and used a multiomic approach. Hence, we arrived at distinct conclusions from another scRNA-seq study of mild-moderate COPD lung tissue (39). Furthermore, we validated our results in a much larger patient cohort. An additional limitation is that we relied on tissue from lung cancer resections. To control for this, we compared both explanted donor lung and "control" lung from surgical cancer resections. Illustrating the need for both comparisons, our analysis demonstrated differences between donor lung and control lung. Furthermore, we selected highly robust findings that were significantly different from both donor and control lung. Second, we were not able to validate whether the increase in $T_{RM}1$ cells was specific to mild-moderate disease. Identification of $T_{RM}1$ cells required both proteomic and transcriptomic markers, and so $T_{RM}1$ cells were not precisely identified in published single-cell or bulk RNA-seq datasets of COPD lung. Multiomic studies of larger sample sizes, including end-stage COPD lungs, could confirm whether CD8^{+} T cell subpopulations correlate with disease activity or severity.

An additional limitation is that we lack information on spatial distribution of CD8^{+} T-cell subpopulations in different stages of COPD lung, which would help inform cell–cell interactions. In addition, functional assessment of isolated CD8^{+} T cells would further advance our understanding of the role of CD8^{+} T-cell subpopulations in COPD pathogenesis. Last, we acknowledge that our cross-species comparison examined only one murine model. *Hhip*$^{+/-}$ mice do develop inflammation and emphysema upon aging and smoking exposure that model elements of clinical COPD (49, 50). In addition, the terminally differentiated KLRG1^{+} T cells in mice are known to have similarities to human TEMRA cells (51). Nevertheless, future comparisons of multiomic analysis of human COPD lung to other murine models, including smoke exposure, are merited.

Conclusions

In summary, our approach demonstrates the value of single-cell, multiomic immunophenotyping of COPD lung tissue. We show that CD8^{+}KLRG1^{+} TEMRA cells have increased relative abundance in mild-moderate COPD lung, and they interact with myeloid and AT2 cells via IFNγ. Validation in a large cohort of patients and cross-species analysis suggest that specific CD8^{+} T cell subpopulations may drive the inflammation in COPD that precedes severe disease, which may have therapeutic implications for slowing the progression of COPD. ■

Author disclosures are available with the text of this article at www.atsjournals.org.

MassGeneralBrigham - Bayer Pulmonary Drug Discovery Laboratory Consortium members Bayer: Markus Koch, Alessandro Arduini, Hana Cernecka, Nicole Schmidt, Alexis Laux-Biehlmann, Damian Brockschnieder, Xiaofei Cong, Anna Engler, Mahmoud Ibrahim, Dhawal Jain, Ivan Kryukov, Kuldeep Kumawat, T. Lang, Yelena Leathurby, Xin Lin, Joerg Meding, Carlos Neideck, Kseniya Obraztsova, C. Pavuluri, Magdalena Platzk, Patrick Smith, Florian Sohler, Salil Srivastava, P. Srinivasa, Tobias Strunz, Jody Sylvia, Lea Vaas, Justus Veerkamp, Alex Zink, Lingyao Zhang, L. Zeng, Xin Lin. Brigham and Women's Hospital (BWH) Channing Division of Network Medicine: Edwin Silverman, Vincent Carey, Peter Castaldi, Michael Cho, Dawn DeMeo, Craig Hersh, Brian Hobbs, Matthew Moll, Heena Rijhwani, Jeong Yun, Xiaobo Zhou. BWH Division of Pulmonary and Critical Care Medicine: Bruce D. Levy, Yohannes Tesfaigzi, Humra Athar, Yan Bai, Rebecca Baron, Tracy Doyle, Souheil El-Chemaly, Laura Fredenburgh, G. Matt Hunninghake, Yunju Jeong, Edy Y. Kim, Nandini Krishnamoorthy, Yohannes Mebratu, Mark Perrella, Joselyn Rojas Quintero, Zerihun Negasi, Mizanur Rahman, Dereje Tassew, Nirmal Sharma, Tomoyoshi Tamura, Ana B. Villaseñor-Altamirano. Massachusetts General Hospital Division of Pulmonary and Critical Care Medicine: Benjamin Medoff, Elizabeth Abe, Katherine Black, Corey Hardin, Rachel Knipe, Barry Shea, Jill Spiney. MassGeneralBrigham: Mahaa Albsuharif, Francesca Giacona, Armin Jayaswai, Greg Keras, Sool Lee, Jianyuan Liu, Chandan Pavuluri, Betty Pham, Samuel Saliba, Pooja Srivastava, Yichao Wang, Shuang Xu.

Acknowledgment: This study was performed as part of the MassGeneralBrigham–Bayer Pulmonary Drug Discovery Laboratory. The Brigham and Women's Hospital Center for Cellular Profiling (co-directed by Kevin Wei and Michael B. Brenner) and its staff (Adam T. Chicoine and Gerald F. Watts) provided flow cytometry and single-cell sequencing expertise. The Brigham and Women's Hospital tissue bank assisted with biobanking of lung tissue. This study used data provided by the Lung Tissue Research Consortium supported by the NHLBI. RNA-sequencing in the Lung Tissue Research Consortium was completed through the NHLBI Trans-Omics for Precision Medicine (TOPMed) project.

References

1. Hogg JC, Chu F, Utokaparch S, Woods R, Elliott WM, Buzatu L, *et al.* The nature of small-airway obstruction in chronic obstructive pulmonary disease. *N Engl J Med* 2004;350: 2645–2653.
2. Barnes PJ. Inflammatory mechanisms in patients with chronic obstructive pulmonary disease. *J Allergy Clin Immunol* 2016; 138:16–27.
3. Hikichi M, Mizumura K, Maruoka S, Gon Y. Pathogenesis of chronic obstructive pulmonary disease (COPD) induced by cigarette smoke. *J Thorac Dis* 2019;11:S2129–S2140.
4. Williams M, Todd I, Fairclough LC. The role of CD8 + T lymphocytes in chronic obstructive pulmonary disease: a systematic review. *Inflamm Res* 2021;70:11–18.
5. Sauler M, McDonough JE, Adams TS, Kothapalli N, Barnthaler T, Werder RB, *et al.* Characterization of the COPD alveolar niche using single-cell RNA sequencing. *Nat Commun* 2022;13:494.

6. Huang Q, Wang Y, Zhang L, Qian W, Shen S, Wang J, *et al.* Single-cell transcriptomics highlights immunological dysregulations of monocytes in the pathobiology of COPD. *Respir Res* 2022;23:367.
7. Madissoon E, Oliver AJ, Kleshchevnikov V, Wilbrey-Clark A, Polanski K, Richoz N, *et al.* A spatially resolved atlas of the human lung characterizes a gland-associated immune niche. *Nat Genet* 2023;55:66–77.
8. Madissoon E, Oliver AJ, Kleshchevnikov V, Wilbrey-Clark A, Polanski K, Ribeiro Orsi AE, *et al.* A spatially resolved atlas of the human lung characterizes a gland-associated immune niche. *Nat. Genet* 2023;55:66–77.
9. Unterman A, Sumida TS, Nouri N, Yan X, Zhao AY, Gasque V, *et al.*; Yale IMPACT Research Team. Single-cell multi-omics reveals dyssynchrony of the innate and adaptive immune system in progressive COVID-19. *Nat Commun* 2022;13:440.
10. Pang J, Qi X, Luo Y, Li X, Shu T, Li B, *et al.* Multi-omics study of silicosis reveals the potential therapeutic targets PGD_2 and TXA_2. *Theranostics* 2021;11:2381–2394.
11. Villaseñor-Altamirano ABB, Jain D, Jeong Y, Athar H, Zhou X, Hersh CP, *et al.* Tissue-resident memory and TEMRA CD8+ T cells in the lungs of patients with mild-moderate COPD. *Am J Respir Crit Care Med* 2023;207:A6201.
12. Korsunsky I, Wei K, Pohin M, Kim EY, Barone F, Major T, *et al.* Cross-tissue, single-cell stromal atlas identifies shared pathological fibroblast phenotypes in four chronic inflammatory diseases. *Med* 2022;3:481–518.e14.
13. McInnes L, Healy J, Melville J. Dimensionality reduction for visualizing single-cell data using UMAP. *Nat. Biotechnol* 2019; 37:38–44.
14. Adams TS, Schupp JC, Poli S, Ayaub EA, Neumark N, Ahangari F, *et al.* Single-cell RNA-seq reveals ectopic and aberrant lung-resident cell populations in idiopathic pulmonary fibrosis. Sci Adv 2020;6:eaba1983.
15. Travaglini KJ, Nabhan AN, Penland L, Sinha R, Gillich A, Sit RV, *et al.* A molecular cell atlas of the human lung from single-cell RNA sequencing. *Nature* 2020;587:619–625.
16. Zappia L, Oshlack A. Clustering trees: a visualization for evaluating clusterings at multiple resolutions. *Gigascience* 2018;7:giy083.
17. Yun JH, Lee C, Liu T, Liu S, Kim EY, Xu S, *et al.* Hedgehog interacting protein-expressing lung fibroblasts suppress lymphocytic inflammation in mice. *JCI Insight* 2021;6:e144575.
18. Ghosh AJ, Hobbs BD, Yun JH, Saferali A, Moll M, Xu Z, *et al.*; NHLBI Trans-Omics for Precision Medicine (TOPMed) Consortium. Lung tissue shows divergent gene expression between chronic obstructive pulmonary disease and idiopathic pulmonary fibrosis. *Respir Res* 2022; 23:97.
19. Hänzelmann S, Castelo R, Guinney J. GSVA: gene set variation analysis for microarray and RNA-seq data. *BMC Bioinformatics* 2013;14:7.
20. Bromley SK, Akbaba H, Mani V, Mora-Buch R, Chasse AY, Sama A, *et al.* Cd49a regulates cutaneous resident memory CD8+ T cell persistence and response. *Cell Rep* 2020;32:108085.
21. Dominguez CX, Amezquita RA, Guan T, Marshall HD, Joshi NS, Kleinstein SH, *et al.* The transcription factors ZEB2 and T-bet cooperate to program cytotoxic T cell terminal differentiation in response to LCMV viral infection. *J Exp Med* 2015;212: 2041–2056.
22. Weinreich MA, Takada K, Skon C, Reiner SL, Jameson SC, Hogquist KA. KLF2 transcription-factor deficiency in T cells results in unrestrained cytokine production and upregulation of bystander chemokine receptors. *Immunity* 2009;31:122–130.
23. Kuo CT, Veselits ML, Leiden JM. LKLF: a transcriptional regulator of single-positive T cell quiescence and survival. *Science* 1997;277: 1986–1990.
24. Buckley AF, Kuo CT, Leiden JM. Transcription factor LKLF is sufficient to program T cell quiescence via a c-Myc-dependent pathway. *Nat Immunol* 2001;2:698–704.
25. Fellows E, Gil-Parrado S, Jenne DE, Kurschus FC. Natural killer cell-derived human granzyme H induces an alternative, caspase-independent cell-death program. *Blood* 2007;110:544–552.
26. Zhang J, Marotel M, Fauteux-Daniel S, Mathieu A-L, Viel S, Marçais A, *et al.* T-bet and Eomes govern differentiation and function of mouse and human NK cells and ILC1. *Eur J Immunol* 2018;48:738–750.
27. Raveney BJE, Sato W, Takewaki D, Zhang C, Kanazawa T, Lin Y, *et al.* Involvement of cytotoxic Eomes-expressing $CD4^+$ T cells in secondary progressive multiple sclerosis. *Proc Natl Acad Sci USA* 2021;118: e2021818118.
28. Chang G-W, Hsiao C-C, Peng Y-M, Vieira Braga FA, Kragten NAM, Remmerswaal EBM, *et al.* The Adhesion G protein-coupled receptor GPR56/ADGRG1 is an inhibitory receptor on human NK cells. *Cell Rep* 2016;15:1757–1770.
29. Kos J, Nanut MP, Prunk M, Sabotič J, Dautović E, Jewett A. Cystatin F as a regulator of immune cell cytotoxicity. *Cancer Immunol Immunother* 2018;67:1931–1938.
30. Milner JJ, Toma C, He Z, Kurd NS, Nguyen QP, McDonald B, *et al.* Heterogenous populations of tissue-resident $CD8^+$ T cells are generated in response to infection and malignancy. *Immunity* 2020;52: 808–824.e7.
31. Jin S, Guerrero-Juarez CF, Zhang L, Chang I, Ramos R, Kuan C-H, *et al.* Inference and analysis of cell-cell communication using CellChat. *Nat Commun* 2021;12:1088.
32. Winkles JA. The TWEAK-Fn14 cytokine-receptor axis: discovery, biology and therapeutic targeting. *Nat Rev Drug Discov* 2008;7:411–425.
33. Browaeys R, Saelens W, Saeys Y. NicheNet: modeling intercellular communication by linking ligands to target genes. *Nat Methods* 2020; 17:159–162.
34. Yang IV, Pedersen BS, Rabinovich E, Hennessy CE, Davidson EJ, Murphy E, *et al.* Relationship of DNA methylation and gene expression in idiopathic pulmonary fibrosis. *Am J Respir Crit Care Med* 2014;190: 1263–1272.
35. Zhou X, Baron RM, Hardin M, Cho MH, Zielinski J, Hawrylkiewicz I, *et al.* Identification of a chronic obstructive pulmonary disease genetic determinant that regulates HHIP. *Hum Mol Genet* 2012;21: 1325–1335.
36. Hobbs BD, de Jong K, Lamontagne M, Bossé Y, Shrine N, Artigas MS, *et al.*; COPDGene Investigators; ECLIPSE Investigators; LifeLines Investigators; SPIROMICS Research Group; International COPD Genetics Network Investigators; UK BiLEVE Investigators; International COPD Genetics Consortium. Genetic loci associated with chronic obstructive pulmonary disease overlap with loci for lung function and pulmonary fibrosis. *Nat Genet* 2017;49:426–432.
37. Li Y, Zhang L, Polverino F, Guo F, Hao Y, Lao T, *et al.* Hedgehog interacting protein (HHIP) represses airway remodeling and metabolic reprogramming in COPD-derived airway smooth muscle cells. *Sci Rep* 2021;11:9074.
38. Rustam S, Hu Y, Mahjour SB, Rendeiro AF, Ravichandran H, Urso A, *et al.* A unique cellular organization of human distal airways and its disarray in chronic obstructive pulmonary disease. *Am J Respir Crit Care Med* 2023;207:1171–1182.
39. Watanabe N, Fujita Y, Nakayama J, Mori Y, Kadota T, Hayashi Y, *et al.* Anomalous epithelial variations and ectopic inflammatory response in chronic obstructive pulmonary disease. *Am J Respir Cell Mol Biol* 2022;67:708–719.
40. Pei Y, Wei Y, Peng B, Wang M, Xu W, Chen Z, *et al.* Combining single-cell RNA sequencing of peripheral blood mononuclear cells and exosomal transcriptome to reveal the cellular and genetic profiles in COPD. *Respir Res* 2022;23:260.
41. Gupta S, Gollapudi S. Effector memory CD8+ T cells are resistant to apoptosis. *Ann N Y Acad Sci* 2007;1109:145–150.
42. Freeman CM, Han MK, Martinez FJ, Murray S, Liu LX, Chensue SW, *et al.* Cytotoxic potential of lung CD8(+) T cells increases with chronic obstructive pulmonary disease severity and with in vitro stimulation by IL-18 or IL-15. *J Immunol* 2010;184:6504–6513.
43. Gupta S, Su H, Bi R, Gollapudi S. Differential sensitivity of naïve and memory subsets of human CD8+ T cells to TNF-alpha-induced apoptosis. *J Clin Immunol* 2006;26:193–203.
44. Fernandes JR, Pinto TNC, Arruda LB, da Silva CCBM, de Carvalho CRF, Pinto RMC, *et al.* Age-associated phenotypic imbalance in TCD4 and TCD8 cell subsets: comparison between healthy aged, smokers, COPD patients and young adults. *Immun Ageing* 2022;19:9.
45. Xiong H, Cui M, Kong N, Jing J, Xu Y, Liu X, *et al.* Cytotoxic $CD161^-CD8^+$ T_{EMRA} cells contribute to the pathogenesis of systemic lupus erythematosus. *EBioMedicine* 2023;90:104507.

46. Shi Z, Wang X, Wang J, Chen H, Du Q, Lang Y, *et al.* Granzyme B + CD8 + T cells with terminal differentiated effector signature determine multiple sclerosis progression. *J Neuroinflammation* 2023; 20:138.
47. Paats MS, Bergen IM, Hoogsteden HC, van der Eerden MM, Hendriks RW. Systemic CD4+ and CD8+ T-cell cytokine profiles correlate with GOLD stage in stable COPD. *Eur Respir J* 2012;40: 330–337.
48. Wang C, Hyams B, Allen NC, Cautivo K, Monahan K, Zhou M, *et al.* Dysregulated lung stroma drives emphysema exacerbation by potentiating resident lymphocytes to suppress an epithelial stem cell reservoir. *Immunity* 2023;56:576–591.e10.
49. Lao T, Jiang Z, Yun J, Qiu W, Guo F, Huang C, *et al.* Hhip haploinsufficiency sensitizes mice to age-related emphysema. *Proc Natl Acad Sci USA* 2016;113:E4681–E4687.
50. Kheradmand F, Zhang Y, Corry DB. Contribution of adaptive immunity to human COPD and experimental models of emphysema. *Physiol Rev* 2023;103:1059–1093.
51. Muroyama Y, Wherry EJ. Memory T-cell heterogeneity and terminology. *Cold Spring Harb Perspect Biol* 2021;13:a037929.